

Takeshi Miyatsuka,<sup>1,2,3</sup> Taka-aki Matsuoka,<sup>3</sup> Shugo Sasaki,<sup>3</sup> Fumiyo Kubo,<sup>3</sup> Ichiro Shimomura,<sup>3</sup> Hiroataka Watada,<sup>1,2</sup> Michael S. German,<sup>4</sup> and Manami Hara<sup>5</sup>



# Chronological Analysis With Fluorescent Timer Reveals Unique Features of Newly Generated $\beta$ -Cells



*Diabetes* 2014;63:3388–3393 | DOI: 10.2337/db13-1312

**Although numerous studies have uncovered the molecular mechanisms regulating pancreas development, it remains to be clarified how  $\beta$ -cells arise from progenitors and how recently specified  $\beta$ -cells are different from pre-existing  $\beta$ -cells. To address these questions, we developed a mouse model in which the insulin 1 promoter drives DsRed-E5 Timer fluorescence that shifts its spectrum over time. In transgenic embryos, green fluorescent  $\beta$ -cells were readily detected by FACS and could be distinguished from mature  $\beta$ -cells only until postnatal day 0, suggesting that  $\beta$ -cell neogenesis occurs exclusively during embryogenesis. Transcriptome analysis with green fluorescent cells sorted by FACS demonstrated that newly differentiated  $\beta$ -cells highly expressed progenitor markers, such as Sox9, Neurog3, and Pax4, showing the progenitor-like features of newborn  $\beta$ -cells. Flow cytometric analysis of cell cycle dynamics showed that green fluorescent cells were mostly quiescent, and differentiated  $\beta$ -cells were mitotically active. Thus, the precise temporal resolution of this model enables us to dissect the unique features of newly specified insulin-producing cells, which could enhance our understanding of  $\beta$ -cell neogenesis for future cell therapy.**

Diabetes results from relative or absolute insulin insufficiency, and as such, considerable effort has been devoted to understanding and controlling the embryonic formation of insulin-secreting cells so that this insufficiency

may be resolved. During embryonic development, islet cells derive from a common Neurog3-expressing progenitor, and mature pancreatic  $\beta$ -cells are defined as glucose-responsive, insulin-secreting cells. Although numerous studies have elucidated the molecular mechanisms of pancreas organogenesis and islet formation (1–3), there is little information on the mechanisms involved in the generation of  $\beta$ -cells from precursors and the differences between recently specified  $\beta$ -cells and preexisting  $\beta$ -cells.

A transgenic mouse model that expresses green fluorescent protein (GFP) under the control of mouse insulin 1 promoter (MIP) has been used extensively to separate the  $\beta$ -cell population from the other islet cell types (4,5). Because all  $\beta$ -cells of MIP-GFP mouse are labeled as green fluorescent cells once the insulin promoter is activated, distinguishing newly specified  $\beta$ -cells from more mature populations with this model is impossible.

## RESULTS

We report a novel mouse model that can circumvent this problem by using a single transgene, MIP-Timer, in which the MIP drives the reporter protein DsRed-E5, a variant of the *Discosoma* species red fluorescent protein that shifts its fluorescence emission peak from green to red in a time-dependent manner (6) (Fig. 1A). Because newly differentiated  $\beta$ -cells have only green fluorophores that have recently been translated under the control of insulin promoter, they are observed as green fluorescent cells

<sup>1</sup>Department of Metabolism and Endocrinology, Juntendo University Graduate School of Medicine, Tokyo, Japan

<sup>2</sup>Center for Molecular Diabetology, Juntendo University Graduate School of Medicine, Tokyo, Japan

<sup>3</sup>Department of Metabolic Medicine, Osaka University Graduate School of Medicine, Osaka, Japan

<sup>4</sup>Diabetes Center, University of California San Francisco, San Francisco, CA

<sup>5</sup>Department of Medicine, The University of Chicago, Chicago, IL

Corresponding author: Takeshi Miyatsuka, miyatsuka-takeshi@umin.net.

Received 25 August 2013 and accepted 6 May 2014.

This article contains Supplementary Data online at <http://diabetes.diabetesjournals.org/lookup/suppl/doi:10.2337/db13-1312/-/DC1>.

© 2014 by the American Diabetes Association. Readers may use this article as long as the work is properly cited, the use is educational and not for profit, and the work is not altered.

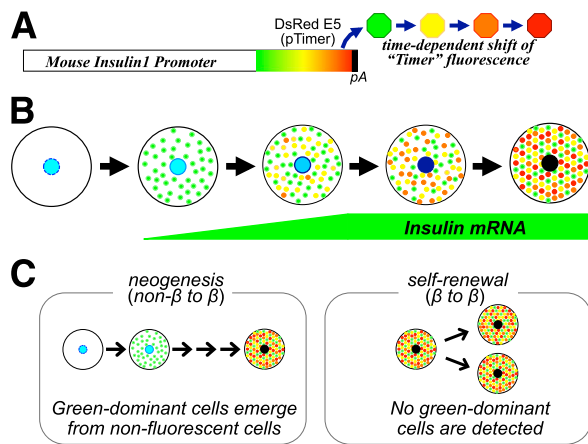


**Figure 1**—Schematic of the MIP-Timer mouse system for sorting early  $\beta$ -cells separately from more-differentiated  $\beta$ -cells. **A:** In MIP-Timer transgenic mice, DsRed-E5 (pTimer) fluorescent protein is expressed under the control of MIP, shifting its emission spectrum from green to red over time. **B:** Because newly specified  $\beta$ -cells have only green fluorophores that have recently been translated, they are observed as green fluorescent cells. As the  $\beta$ -cell differentiates, yellow and then red fluorescent molecules appear intracellularly. **C:** Thus, only  $\beta$ -cells that have recently been generated from their progenitors are observed as green fluorescent cells. When  $\beta$ -cells are supplied by self-renewal, they are never detected as green-dominant cells, having a substantial number of red fluorophores.

(Fig. 1B). As the  $\beta$ -cell matures, it contains both yellow and red fluorescent DsRed-E5 molecules as well as recently translated green molecules and, therefore, exhibits a yellow-to-orange fluorescent signal, representing the sum of various ages of fluorophores (Fig. 1B). When  $\beta$ -cells are supplied by self-renewal, they are never detected as green-dominant cells because a substantial amount of mature red-emitting DsRed-E5 is shared between newly divided cells (Fig. 1C). Thus, this model facilitates separation of the earliest green fluorescent  $\beta$ -cells from other fluorescent populations.

In MIP-Timer transgenic embryos and neonates, both green and red fluorescent signals were readily detected by both flow cytometry and fluorescent microscopy (Fig. 2A and Supplementary Fig. 1), and all fluorescent proteins overlapped with cells containing insulin immunoreactivity. The green fluorescent cells were detected by flow cytometry, whereas only green/red double-positive cells were observed by fluorescent microscopy, consistent with findings by Bertera et al. (7) and by ourselves with Neurog3-Timer mice (8). This is probably because the number of green fluorophores in the earliest  $\beta$ -cells is too small to reach the detection sensitivity of fluorescence microscopy as a result of the lower activity of MIP in early  $\beta$ -cells. Furthermore, flow cytometric analysis revealed that  $\sim 1\%$  of the whole pancreatic cells between E15.5 and E18.5 were green fluorescent (i.e., recently generated  $\beta$ -cells) (Fig. 2B). After postnatal day 1, the proportion of green-dominant fluorescent cells declined dramatically (to  $<0.02\%$ ), and almost all fluorescent cells were green/red double positive (Fig. 2C). In addition, no green-dominant cells were

observed when  $\beta$ -cell regeneration/expansion was induced during pregnancy or in the diabetic state created by treatment with streptozotocin (Supplementary Fig. 2A and B). These findings are consistent with previous observations showing that adult  $\beta$ -cells maintain their mass predominantly through the replication of preexisting  $\beta$ -cells rather than being newly formed from progenitor cells (9–13). On the other hand, when the transcription factors Pdx1, Neurog3, and Mafa that induce acinar-to- $\beta$  reprogramming (14) were introduced by adenovirus injection into the pancreatic tail of adult MIP-Timer mice, green-dominant cells were clearly observed 4 days after the adenovirus injection only in the pancreatic tail where the adenoviruses were injected (Supplementary Fig. 3). These results show that the MIP-Timer system enables one to distinguish the earliest  $\beta$ -cells from the other populations in the adult stage as well as during embryonic development.

To investigate the characteristics of  $\beta$ -cells in a time-dependent manner, the cells of E16.5 MIP-Timer pancreata were sorted by FACS into three populations shown in Fig. 2D (i.e., early  $\beta$ -cells, late  $\beta$ -cells, non- $\beta$ -cells), and real-time PCR analyses were performed for endocrine hormones and an exocrine enzyme. Expression levels of insulin mRNA were sequentially upregulated during  $\beta$ -cell maturation (Fig. 2E and F). Both early and late  $\beta$ -cells exhibited significantly higher expression levels for endocrine hormones and lower levels for pancreatic-type amylase 2a5 than non- $\beta$ -cells (Fig. 2G–K). Of note, the expression levels for somatostatin, pancreatic polypeptide, and ghrelin were significantly higher in the early  $\beta$ -cells than in the late  $\beta$ -cells and non- $\beta$ -cells, suggesting that at least a proportion of early  $\beta$ -cells express other endocrine hormones, but they lose such expression with further differentiation.

To further characterize these cell populations by gauging the expression of known pancreatic transcriptional regulators, TaqMan RT-PCR assays were performed with RNAs from the cells isolated by FACS from E16.5 MIP-Timer pancreata in the same manner as shown in Fig. 2D. Among 65 transcriptional regulators, Sox9, Neurog3, Pax4, and Arx, all of which are known to play roles in progenitor populations and are suppressed in mature  $\beta$ -cells, demonstrated an expression peak in the early  $\beta$ -cell population (Fig. 3A–D and Supplementary Table 1). In addition, Hes1 and Onecut1, which have been shown to function upstream of endocrine progenitors, were highly expressed in the early  $\beta$ -cells and non- $\beta$ -cell populations but significantly downregulated in the late  $\beta$ -cells (Fig. 3E and F). These findings suggest undifferentiated features of the earliest  $\beta$ -cells consistent with the unexpected expression of other endocrine hormones shown in Fig. 2G–J. In contrast, Mafa and Hopx exhibited the highest expression levels in late  $\beta$ -cells (Fig. 3G and H), whereas Pdx1, Neurod1, Nkx2-2, and Nkx6-1 showed comparable expression in early and late  $\beta$ -cell populations (Fig. 3I–L), which may imply important roles of Mafa and Hopx in the final maturation of  $\beta$ -cells.

Whereas insulin 1 and 2 were expressed only at low levels in the earliest  $\beta$ -cells (Fig. 2E and F), the genes

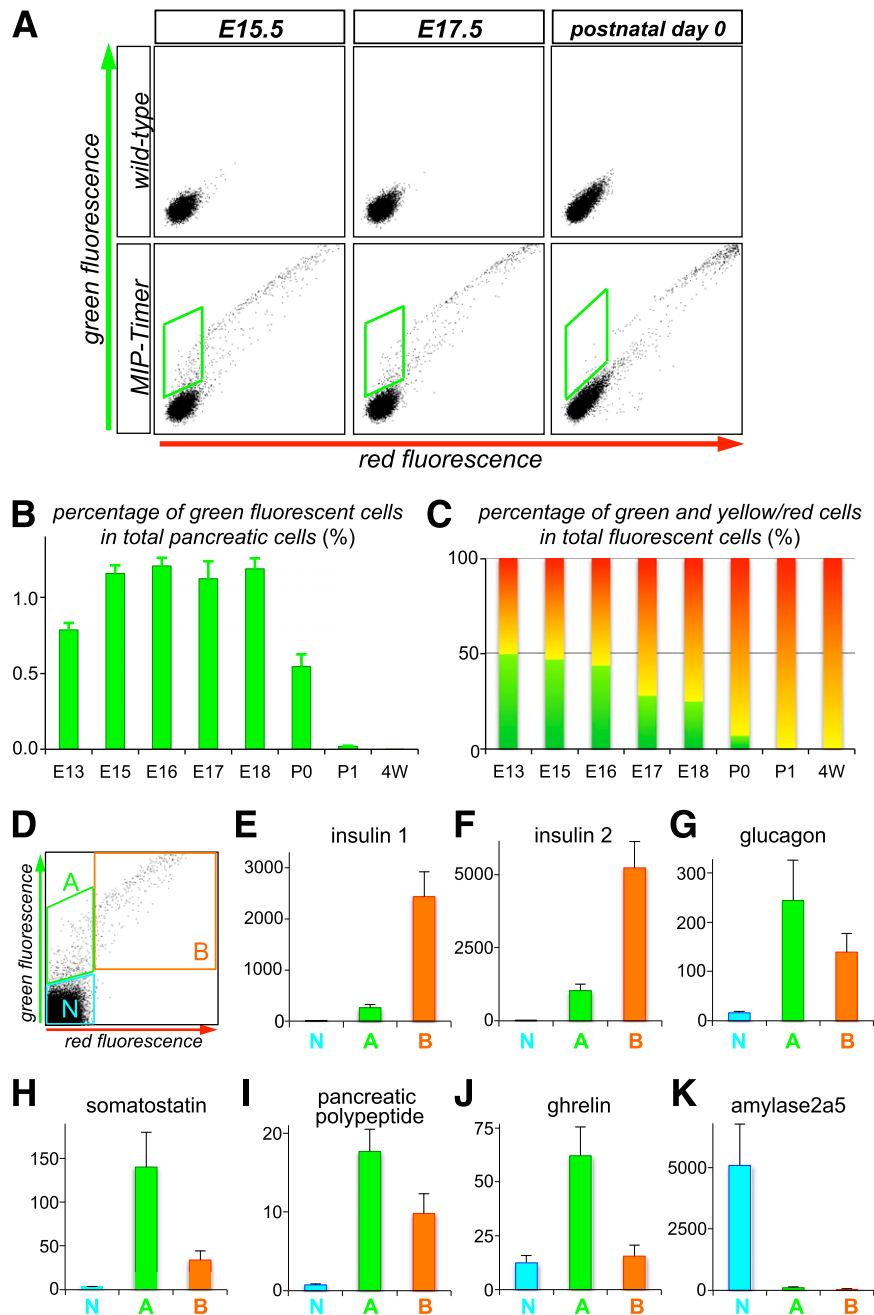


**Figure 2**—Fluorescent patterns in developing pancreata of MIP-Timer mice and mRNA expression profiles for pancreas-specific genes. *A*: Pancreata from wild-type (*top panels*) and MIP-Timer mice (*bottom panels*) were dissociated at E15.5 and E17.5 and at postnatal day 0 (P0) and analyzed using flow cytometry. *B*: Percentage of green fluorescent cells among total pancreatic cells. *C*: Relative numbers of green and yellow/red cells. *D*: MIP-Timer pancreata were dissected at E16.5 and sorted by FACS into three gates (N, non- $\beta$ -cells; A, early  $\beta$ -cells; B, late  $\beta$ -cells). The sorted cell populations were analyzed by real-time RT-PCR for mRNA encoding endocrine hormones (*E–J*) and exocrine enzyme (*K*). All expression levels were normalized to  $\beta$ -glucuronidase. Data in *B* and *E–K* are mean  $\pm$  SE of at least four samples.

related to glucose-stimulated insulin secretion, such as ABCC8 (SUR) and Kcnj11 (Kir6.2), were highly expressed in both early and late  $\beta$ -cell populations (Supplementary Fig. 4 and Supplementary Table 1). It is noted that glucokinase (Gck), a high-K<sub>m</sub> hexokinase isoform, is expressed in the earliest  $\beta$ -cells at a level that is as high as in mature  $\beta$ -cells. In contrast, the low-K<sub>m</sub> hexokinase isoforms Hk2, Ldha, and Slc16a1 (also known as Mct1 [monocarboxylate

transporter isoform 1]), which play roles in anaerobic glycolysis and are expressed in many other tissues (15,16), were repressed in the earliest and mature  $\beta$ -cells. These findings imply that  $\beta$ -cells start to acquire some features responsible for glucose-stimulated insulin secretion at a very early stage of  $\beta$ -cell specification.

We reported previously that most endocrine progenitors are quiescent after the initiation of Neurog3

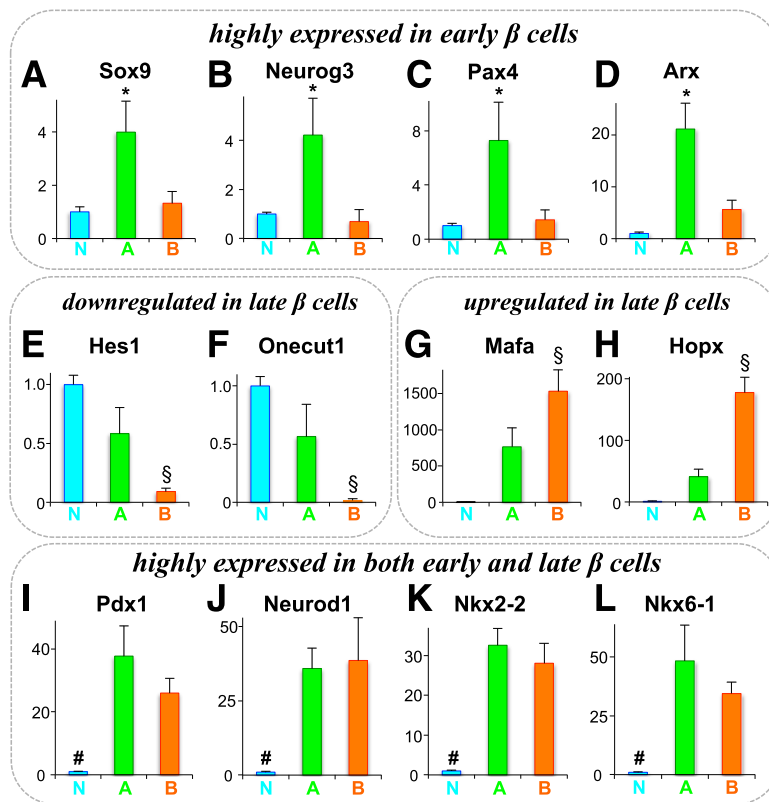


**Figure 3**—Temporal transcriptome analysis for transcriptional regulators in MIP-Timer embryos. The pancreata of MIP-Timer embryos were dissected at E16.5 and sorted by FACS into three gates (N, non- $\beta$ -cells; A, early  $\beta$ -cells; B, late  $\beta$ -cells). The sorted cell populations were analyzed by real-time RT-PCR for mRNAs encoding transcriptional regulators (A–L). All expression levels were normalized to  $\beta$ -glucuronidase. Expression levels are shown relative to the level in gate N. Data are mean  $\pm$  SE of four independent experiments. \* $P$  < 0.05 vs. population N and B; § $P$  < 0.05 vs. population N and A; # $P$  < 0.05 vs. population A and B.

expression and then differentiated endocrine cells, including  $\beta$ -cells, reenter the cell cycle during late fetal development (17,18). However, it remains to be determined whether the differentiation status of  $\beta$ -cells affects timing of cell proliferation. To address this question, the cell cycle status during  $\beta$ -cell maturation was analyzed by flow cytometry using E18.5 MIP-Timer embryos stained with the DNA dye Hoechst 33342. As shown in Fig. 4, 8.7% of non- $\beta$ -cells (gate N in Fig. 2D) were proliferating in S/G<sub>2</sub>/M phase, whereas >99% of early  $\beta$ -cells (gate A) were in G<sub>0</sub>/G<sub>1</sub> phase (Fig. 4A and B), demonstrating that newly generated  $\beta$ -cells were quiescently similar to the endocrine progenitors expressing Neurog3 (18). On the other hand, >5% of the late  $\beta$ -cells (gate B) were in S/G<sub>2</sub>/M phase. Of note, when the differentiated  $\beta$ -cells in gate B were divided equally into three populations according to their red fluorescent intensity, one-third of the  $\beta$ -cells with the highest fluorescent intensity (gate B<sup>hi</sup>) were most frequently proliferating; >10% of mature  $\beta$ -cells were in S/G<sub>2</sub>/M phase (Fig. 4C and D), indicating that a certain period of time is required (>6 h) until  $\beta$ -cells acquire high self-renewal capacity. Because green/red double-fluorescent cells comprise differentiated  $\beta$ -cells of varying ages (several hours to days), another chronological method

is required to clarify the exact stage at which  $\beta$ -cells actually reenter the cell cycle.

## DISCUSSION

Thus, this MIP-Timer mouse is an efficient tool for dissecting and characterizing the earliest  $\beta$ -cells separately from more-differentiated  $\beta$ -cells. Xiao et al. (9) recently reported that the Cre-loxP-mediated isolation system can be used for labeling early  $\beta$ -cells, demonstrating no evidence of  $\beta$ -cell neogenesis in adult pancreata, which is comparable with the present finding shown in Fig. 2B. On the other hand, whereas the Cre-loxP system continues to detect early  $\beta$ -cells until postnatal day 5, the MIP-Timer transgenic mouse detected little  $\beta$ -cell neogenesis after postnatal day 0. This 5-day difference is likely due to both the significant time lag between Cre expression and reporter gene expression after Cre-mediated recombination, which had been estimated at 40–48 h in Xiao et al., and the sustained expression of the red fluorescent protein (mTomato), which delays the detection of green-only cells. One advantage of our system, therefore, is that it is based on a single fluorescent protein with a short (6-h) maturation window (8). The difference in temporal resolution between these studies likely results in different

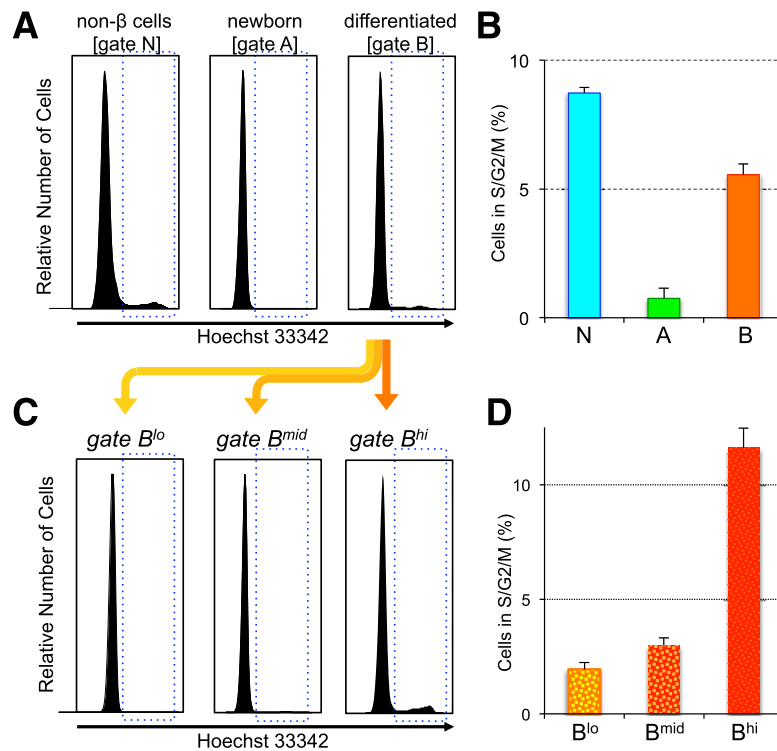


**Figure 4**—Proliferation during  $\beta$ -cell neogenesis and maturation. **A:** Dissociated cells from E17.5 MIP-Timer embryos were stained with the DNA-specific dye Hoechst 33342 and analyzed by flow cytometry for the three different populations shown in Fig. 2D. **B:** Percentage of proliferating cells at S/G<sub>2</sub>/M phases for each population (N, non- $\beta$ -cells; A, early  $\beta$ -cells; B, late  $\beta$ -cells). Data are mean  $\pm$  SE of three samples. **C:** Differentiated  $\beta$ -cells in gate B were divided equally into three populations according to the intensity of red fluorescence. **D:** One-third of  $\beta$ -cells with the highest fluorescent intensity (gate B<sup>hi</sup>) showed the highest proliferation rate compared with the other two-thirds of  $\beta$ -cells in gate B with lower fluorescence (gate B<sup>lo</sup> and B<sup>mid</sup>). Data are mean  $\pm$  SE of three embryos.

expression profiles of pancreas-specific genes in early  $\beta$ -cells. For example, Xiao et al. demonstrated that the early  $\beta$ -cells in the Cre-loxP system expressed the same levels of insulin and Neurog3 as the more-differentiated  $\beta$ -cells; however, our study showed that the early  $\beta$ -cells expressed a higher level of Neurog3 and a lower level of insulin than the mature  $\beta$ -cells. Our model seems to indicate that newly generated  $\beta$ -cells have unique gene expression programs. Further omics approaches for the earliest  $\beta$ -cells in our MIP-Timer mice will lead to a better understanding of the molecular mechanisms underlying  $\beta$ -cell neogenesis and maturation.

## RESEARCH DESIGN AND METHODS

### Generation of MIP-Timer Transgenic Mouse

The MIP-DsRed-E5 (Timer) transgenic construct was assembled using an 8.5-kb fragment of the MIP that includes a region from  $-8.5$  to  $+12$  bp (relative to the transcriptional start site), the DsRed-E5 coding region (pTimer; Clontech, Palo Alto, CA), and a 2.1-kb fragment of the human growth hormone cassette gene. The purified transgene DNA was microinjected into the pronuclei of CD-1 mice by the Transgenic Mouse/ES Core Facility of The University of Chicago Diabetes Research and Training Center. The mice were genotyped by PCR, using the forward primer 5'-AGTTCAGTACGGCTCCAAG-3' and the

reverse primer 5'-CAGCCATGGTCTTCTTCTG-3' in the coding region of DsRed-E5. Mice were housed in a controlled climate on a 12-h light-dark cycle. Timed matings were carried out, with E0.5 being set as midday of the day of discovery of a vaginal plug. All studies involving mice were approved by the University of California, San Francisco, Institutional Animal Care and Use Committee.

### Whole-Mount Observation and Histological Examination

Transgenic MIP-Timer embryos were killed, and macroscopic appearance and fluorescence of the MIP-Timer mice were examined with a fluorescent dissecting microscope. For histological analysis, tissues from 3-week-old MIP-Timer mice were fixed in 4% paraformaldehyde in PBS at 4°C, washed in PBS alone, then immersed into sucrose solution in PBS overnight at 4°C. The next day, the tissues were embedded and frozen in Tissue-Tek O.C.T. Compound (Sakura). Tissues were sectioned at 6- $\mu$ m thickness, permeabilized with 0.1% Triton X-100, and incubated with guinea pig anti-insulin antibody (Dako, Carpinteria, CA) diluted 1:2,000 in PBS and then visualized by using Alexa Fluor 647 anti-guinea pig IgG (Molecular Probes, Eugene, OR).

### Pancreatic Cell Dispersion and Flow Cytometry

The MIP-Timer transgenic mice were distinguished from control littermates using a fluorescent dissecting microscope, and whole pancreata were dissected manually from

other organs. Pancreata were treated with 0.05% trypsin in 0.53 mmol/L EDTA (Invitrogen, Carlsbad, CA) at 37°C for 5 min, and digestion was inactivated by the addition of FBS. The dissociated cells were resuspended in FACS buffer (2% FBS in PBS) and then analyzed using an LSR II flow cytometer (PerkinElmer) or sorted using a MoFlo cell sorter (Dako Cytomation). Dead cells were excluded with DNA dye TO-PRO-3 (Molecular Probes). For cell cycle analysis, the dissociated cells were incubated in a medium containing 5  $\mu$ g/mL Hoechst 33342 dye at 37°C for 60 min, washed with cold PBS, and analyzed with an LSR II flow cytometer.

### Real-Time Quantitative PCR

The cells were sorted by FACS with E16.5 MIP-Timer embryos from four independent experiments. Total RNA was extracted from the sorted cell populations using the RNeasy Plus Micro Kit (Qiagen, Valencia, CA) according to the manufacturer's protocol. The quality and quantity of extracted RNA were assessed with the Agilent 2100 Bioanalyzer using the RNA 6000 Pico Assay Kit (Agilent Technologies, Santa Clara, CA). Next, 10 ng of the total RNA were linearly amplified and converted into cDNA with the NuGEN WT-Ovation RNA Amplification System (NuGEN, San Carlos, CA). Individual cDNAs were quantified by real-time PCR using a TaqMan Low-Density Array system (Applied Biosystems, Foster City, CA) designed for pancreas-specific genes, including endocrine hormones and transcription factors. Gene expression levels of the assayed genes were normalized to the expression levels of  $\beta$ -glucuronidase. Data are expressed as mean  $\pm$  SE.

**Acknowledgments.** The authors thank Francis Lynn (The University of British Columbia), Hail Kim (Korea Advanced Institute of Science and Technology), Hideaki Kaneto (Kawasaki Medical University), and Yoshio Fujitani (Juntendo University) for helpful advice and criticism and Shuwei Jiang (University of California, San Francisco) and Satomi Takebe (Osaka University Graduate School of Medicine) for help with the experiments.

**Funding.** This work was supported by JDRF Advanced Postdoctoral Fellowship award 10-2010-561 and Japan Society for the Promotion of Science KAKENHI No. 25461348.

**Duality of Interest.** H.W. has received lecture fees from Daiichi Sankyo, Takeda, MSD, Sanofi-Aventis, Ono, Novartis, Astellas Pharma, Dainippon Sumitomo Pharma, Mitsubishi Tanabe Pharma, Novo Nordisk, and Sanwa Kagaku Kenkyusho and research funding from Sanofi-Aventis, Novo Nordisk, Novartis, AstraZeneca, Sanwa Kagaku Kenkyusho, Ono, MSD, Boehringer Ingelheim, Kissei, Takeda, Daiichi Sankyo, and Eli Lilly. No other potential conflicts of interest relevant to this article were reported.

**Author Contributions.** T.M. contributed to the study design, flow cytometry analysis, and writing of the manuscript. T.-a.M., I.S., H.W., and M.S.G.

contributed to the discussion and review of the manuscript. S.S. contributed to the in vivo experiments and flow cytometry analysis. F.K. contributed to the in vivo experiments. M.H. generated the transgenic mouse line and contributed to the discussion. T.M. is the guarantor of this work and, as such, had full access to all the data in the study and takes responsibility for the integrity of the data and the accuracy of the data analysis.

### References

- Ackermann AM, Gannon M. Molecular regulation of pancreatic  $\beta$ -cell mass development, maintenance, and expansion. *J Mol Endocrinol* 2007;38:193–206
- Zaret KS. Genetic programming of liver and pancreas progenitors: lessons for stem-cell differentiation. *Nat Rev Genet* 2008;9:329–340
- Puri S, Hebok M. Cellular plasticity within the pancreas—lessons learned from development. *Dev Cell* 2010;18:342–356
- Hara M, Wang X, Kawamura T, et al. Transgenic mice with green fluorescent protein-labeled pancreatic  $\beta$ -cells. *Am J Physiol Endocrinol Metab* 2003;284:E177–E183
- Katsuta H, Akashi T, Katsuta R, et al. Single pancreatic beta cells co-express multiple islet hormone genes in mice. *Diabetologia* 2010;53:128–138
- Terskikh A, Fradkov A, Ermakova G, et al. “Fluorescent timer”: protein that changes color with time. *Science* 2000;290:1585–1588
- Bertera S, Geng X, Tawadrous Z, et al. Body window-enabled in vivo multi-color imaging of transplanted mouse islets expressing an insulin-Timer fusion protein. *Biotechniques* 2003;35:718–722
- Miyatsuka T, Li Z, German MS. Chronology of islet differentiation revealed by temporal cell labeling. *Diabetes* 2009;58:1863–1868
- Xiao X, Chen Z, Shiota C, et al. No evidence for  $\beta$  cell neogenesis in murine adult pancreas. *J Clin Invest* 2013;123:2207–2217
- Dor Y, Brown J, Martinez OI, Melton DA. Adult pancreatic  $\beta$ -cells are formed by self-duplication rather than stem-cell differentiation. *Nature* 2004;429:41–46
- Teta M, Rankin MM, Long SY, Stein GM, Kushner JA. Growth and regeneration of adult  $\beta$  cells does not involve specialized progenitors. *Dev Cell* 2007;12:817–826
- Furuyama K, Kawaguchi Y, Akiyama H, et al. Continuous cell supply from a Sox9-expressing progenitor zone in adult liver, exocrine pancreas and intestine. *Nat Genet* 2011;43:34–41
- Solar M, Cardalda C, Houbracken I, et al. Pancreatic exocrine duct cells give rise to insulin-producing  $\beta$  cells during embryogenesis but not after birth. *Dev Cell* 2009;17:849–860
- Zhou Q, Brown J, Kanarek A, Rajagopal J, Melton DA. In vivo reprogramming of adult pancreatic exocrine cells to  $\beta$ -cells. *Nature* 2008;455:627–632
- Quintens R, Hendrickx N, Lemaire K, Schuit F. Why expression of some genes is disallowed in  $\beta$ -cells. *Biochem Soc Trans* 2008;36:300–305
- Schuit F, Van Lommel L, Granvik M, et al.  $\beta$ -cell-specific gene repression: a mechanism to protect against inappropriate or maladjusted insulin secretion? *Diabetes* 2012;61:969–975
- Nekrep N, Wang J, Miyatsuka T, German MS. Signals from the neural crest regulate beta-cell mass in the pancreas. *Development* 2008;135:2151–2160
- Miyatsuka T, Kosaka Y, Kim H, German MS. Neurogenin3 inhibits proliferation in endocrine progenitors by inducing Cdkn1a. *Proc Natl Acad Sci U S A* 2011;108:185–190